Author Manuscript

Author Manuscript

Author Manuscript

Author Manuscript

HHS Public Access

Author manuscript

J Biomed Mater Res A. Author manuscript; available in PMC 2019 August 01.

Published in final edited form as:

J Biomed Mater Res A. 2016 October ; 104(10): 2604–2615. doi:10.1002/jbm.a.35795.

Enhanced osteoprogenitor elongated collagen fiber matrix formation by bioactive glass ionic silicon dependent on Sp7 (osterix) transcription

Venu G. Varanasi[1], **Tetsurou Odatsu**[2], **Timothy Bishop**[3], **Joyce Chang**[3], **Jeremy Owyoung**[3], **Peter M. Loomer**[4]

[1]Department of Biomedical Sciences, Texas A&M College of Dentistry, Dallas, Texas 75246

[2]Department of Applied Prosthodontics, Graduate School of Biomedical Sciences, Nagasaki University, 1-7-1, Sakamoto, Nagasaki 852-8588, Japan

[3]Division of Periodontology, University of California, San Francisco, California 94143

[4]Department of Periodontology and Implant Dentistry, College of Dentistry, New York University, New York, New York 10010

Abstract

Bioactive glasses release ions, those enhance osteoblast collagen matrix synthesis and osteogenic marker expression during bone healing. Collagen matrix density and osteogenic marker expression depend on osteogenic transcription factors, (e.g., Osterix (OSX)). We hypothesize that enhanced expression and formation of collagen by Si^{4+} depends on enhanced expression of OSX transcription. Experimental bioactive glass (6P53-b) and commercial Bio-glass™ (45S5) were dissolved in basal medium to make glass conditioned medium (GCM). ICP-MS analysis was used to measure bioactive glass ion release rates. MC3T3-E1 cells were cultured for 20 days, and gene expression and extracellular matrix collagen formation was analyzed. In a separate study, siRNA was used to determine the effect of OSX knock-down on impacting the effect of Si^{4+} on osteogenic markers and matrix collagen formation. Each bioactive glass exhibited similar ion release rates for all ions, except Mg^{2+} released by 6P53-b. Gene expression results showed that GCM markedly enhanced many osteogenic markers, and 45S5 GCM showed higher levels of expression and collagen matrix fiber bundle density than 6P53-b GCM. Upon knockdown of OSX transcription, collagen type 5, alkaline phosphatase, and matrix density were not enhanced as compared to wild type cells. This study illustrates that the enhancement of elongated collagen fiber matrix formation by Si^{4+} depends on OSX transcription.

Keywords

bioactive glass; silicon; magnesium; collagen type I; bone regeneration

Correspondence to: V. G. Varanasi; varanasi@bcd.tamhsc.edu.

Author Manuscript Author Manuscript Author Manuscript Author Manuscript

INTRODUCTION

Ti/Ti-alloy implants are becoming increasingly used for structural bone restoration in patients suffering from severe bone loss or injury. Upon implantation, the implant is used to mechanically support the surrounding bone. However, these materials have limited lifetimes because they do not facilitate biological mineral ingress.[1] Because of the poor attachment, the incidence of inflammation and fibrosis can increase.[2] This can cause eventual implant loosening and probable rejection, thus, a “bone-like” surface modification could improve implant-bony attachment.

Previous attempts to coat Ti to facilitate fewer rejections have not greatly improved their bony attachment. Two examples of such attempts include hydroxyapatite (HA)[3–7] and Bioglass™.[8] HA coatings on Ti showed enhanced mineral attachment to the applied layer, however, catastrophic failure occurred at the Ti-mineral interface.[9–15] This failure was mainly due to the poor quality of HA formed by the plasma spray process. The mineral layer that results was highly soluble (22–62% amorphous calcium phosphate) and incorporated multiple calcium phosphate phases (in addition to the HA overlay).[16–23] Hench and colleagues[24] developed a glass material that releases calcium and phosphate ions to cells (as raw materials for osteoblast mineralization) while forming a bone-like HA surface for mineralized tissue attachment. However, coatings involving Bioglass resulted in delamination at the metal-glass/ceramic interface. This delamination was owed to cracking of the glass during the coating process and thermal expansion mismatch between Bioglass™ and Ti.[25]

By modifying the composition of commercial Bioglass™, family of bioactive glasses (50–59 wt % SiO_2) that can be used to form a functionally graded interface between the implant and bone has been developed.[26] These materials form a thin and adherent Ti–Si bond between the glass and TiO_2 layer during an enameling process.[26–28] The bioactive features that define the bioactivity of the glass matrix are its ability to form a hydroxyapatite surface layer and the release of ions to cells for mitogenic activity.[29] These newer bioactive glasses could provide the same bioactive features as commercial Bioglass,[30] while also adhering well to Ti even during loading conditions. Therefore, the effect that these newer glasses have on osteogenesis will be explored here.

For long-term osteointegration, these materials must stimulate and support newly formed bone. Stimulation involves the up-regulation of collagenous, enzymatic, and matrix molecules that promote collagen and bone matrix development. Matrix enzymes, such as alkaline phosphatase, lysil oxidase, and matrix metaloproteineases, are expressed to convert the collagen matrix into a form amenable for matrix protein and mineral incorporation. Table I lists several of these markers involved in osteogenesis. More recent finding have shown that antioxidant metalloenzymes, such as superoxide dismutase (Sod1),[41] are involved in the mechanisms of collagen cross-linking enzymes.[43] If these materials are to be a successful coating for Ti implants, they must stimulate new bone formation by stimulating the expression of these biomarkers and enhancing the density of collagenous matrices during osteogenesis.

Author Manuscript Author Manuscript Author Manuscript Author Manuscript

It has been speculated that Si^{4+} plays a role during collagen matrix synthesis. Collagens are critical for the proper formation of tissues and organs in our body. Type I collagen (Col(I)) is the fibrillar collagen comprising up to 90% of the collagens found in bone.[44] Type V collagen (Col(V)) is a member of the fibrillar collagen group and is present in tissues where Col(I) is present. Col(V) is involved in the control of collagen fibril dimension (diameter) and assembly of collagen matrix.[45] In our previous results[30,46] as well as reports by others[47,48] Si^{4+} (released as an ionic product €from bioactive glasses) was linked to enhanced Col(I) expression, collagen matrix formation, and mineralized tissue formation. Interestingly, collagen fiber bundles were found to be dense, elongated, and thick when osteoblast-like cells were exposed to Si^{4+}.[49] Yet, determination of the mechanistic role that Si^{4+} has on osteogenesis is still needed to isolate a Si^{4+} dose that maximally up-regulates collagen and other osteogenic markers.

To better understand the impact of Si^{4+} on collagen synthesis, a closer examination of up-stream osteogenesis regulators is needed. One such upstream regulator, Osterix (OSX/SP7), is a zinc finger-containing transcription factor belonging to the Sp/KLF (Kruppel Like Factor) family of transcription factors involved in bone development.[50] It is distinctly expressed in osteoblasts and in all developing bones and is essential for the commitment of preosteoblastic cell differentiation into a mineralizing phenotype.[50] OSX triggers downstream expression of other collagenous (Col(V)) and noncollagenous (ALP) markers that indicate the mineralizing osteoblast phenotype.[51,52] Furthermore, it has been reported that OSX upregulates collagen matrix density during osteoblast differentiation.[53] Osteoblast differentiation has been shown to be arrested in OSX null mice, resulting in the absence of bone formation.[54] Overall, current studies indicate the indispensable role of OSX in osteogenesis. However, no study to date has determined if Si^{4+} enhances collagen matrix density via enhanced osteogenic regulators, such as OSX, and this will be studied here.

Thus, we will test the hypothesis that bioactive glasses release ions that enhance osteogenic marker expression and elongated collagen matrix density via Si^{4+} enhancement of osterix osteogenic transcription. The aims of this study are to (1) determine the effect of bioactive glass ionic products of dissolution on osteogenic marker expression and collagen matrix densification and (2) determine if such enhancement depends on Si^{4+} enhancement of osterix transcription factor expression. The goal of this study is to demonstrate that osterix gene expression is required for Si^{4+} enhancement of elongated collagen matrix density.

MATERIALS AND METHODS

Study design

Pertaining to the above aims, particles of bioactive glass (45S5 and 6P53-b) were dissolved in cell culture medium. The glass conditioned medium (GCM) were measured for ion concentrations using inductively coupled plasma mass spectrometry (ICP-MS). Each GCM and control medium was added to differentiating MC3T3-E1 osteoblasts. Cells were cultured for 20 days, and extracted for RNA to measure gene expression using quantitative polymerase chain reaction (qPCR). In parallel studies, cell layers were stained histologically for ECM collagen matrix formation. Statistical comparisons were made between each GCM and control treatment. For the second aim, OSX-null and wild type control osteoblasts were

Author Manuscript Author Manuscript Author Manuscript Author Manuscript

studied to elucidate the possible mechanistic effect of Si^{4+}. The Osterix gene in MC3T3-E1 cells was inhibited using siRNA. Gene expression and histological staining were conducted as described above for OSX and collagen expression.

GCM preparation

Melt-derived experimental bioactive glass (6P53-b) and commercial Bioglass (45S5) were used in this study. The bioactive glass powder specimens were commercially purchased in a specific particle size range of 100–300 μm (Mo-Sci Specialty Products L.L.C., North Rolla, MO). The glass particles were soaked in alpha-minimum essential medium (α-MEM, Invitrogen, Carlsbad, CA for 72 h at 0.016 g mL^{-1} in an incubator (37°C, 5% CO_2, 100% RH). These ion extracts were collected, sterile filtered (0.2 mm), and measured for pH changes using a standard pH meter while ion concentrations were measured using ICP-MS. Each ion extract was then supplemented (by volume) with 10% fetal bovine serum (FBS) and 1% penicillin-streptomycin (pen-strep), 50 ppm ascorbic acid, and 10 mM glycerol-2-phosphate to make 45S5 and 6P53-b GCM.

ICP-MS

Ion extract samples were diluted 1:100 in 3% nitric acid. Ion concentrations were measured as described previously[30] and performed at the University of California ICP-MS Facility in Davis, CA using a 250 amu range ICP-MS machine (Agilent Technologies, Palo Alto, CA).

Cell culture

Prior to experiments, cells (MC3T3-E1 subclone 4, ATCC, Manassas, VA) were grown in control media and in 150 cm^2 flasks to obtain the desired amount of cells for experiments. Cells were expanded to passage 25–30 with media changes every 2–3 days. Cells were pelleted, counted (using a standard hemacytometer and an optical microscope (Nikon TE300, Nikon Inc., Tokyo, Japan)), and seeded (50,000 cells cm^{-2}) into six-well plates. The cells were allowed to attach and then synchronized (using α-MEM, 1% FBS, 1% pen-strep) for 48 h.

Experiments were initiated by exchanging synchronization media with GCM and control treatments. All treatments were further supplemented with AA (50 ppm) and β-GP (10 mM) to induce differentiation. A parallel experiment was conducted in which cells were cultured on glass cover slips (not bioactive glasses) for histological staining. Several time points were used over the course of osteoblast differentiation (~30 days).

qRT-PCR

In quantifying levels of gene expression, qPCR was used. Cells cultured in each treatment were lysed at the time points specified above to collect mRNA (RNeasy Mini Kit, Qiagen, Valencia, CA) and converted to cDNA using reverse transcriptase (Reverse Transcription System, Promega, Madison, WI). A full-spectrum UV–vis nanodrop volumetric analyzer (ND-1000, Nanodrop Technologies, Wilmington, DE) was used to obtain the absorbance (A) measurements of mRNA and cDNA samples. The mRNA and cDNA concentrations were measured at 260 nm (A_{260}) and a nucleic acid absorbance at A_{260}/A_{280} (1.8–2.1) was used

Author Manuscript Author Manuscript Author Manuscript Author Manuscript

to determine quality of samples (advised by manufacture's protocol). cDNA samples were all diluted to a concentration of 100 ng μL^{-1} prior to PCR amplification.

After conversion, cDNA samples were prepared for amplification with the following reagents in these specified concentrations (final concentration): cDNA sample (10% by volume), FastStart Taqman Master Mix (Rox, 2×, 50%) (Roche Applied Sciences, Mannheim, Germany), forward primer (900 n*M*), reverse primer (900 n*M*), and hydrolysis probe (250 n*M*), and PCR grade water (Amgen, South San Francisco, CA). All reaction volumes did not exceed 10 μL. Reactions were executed using a real-time PCR machine (ABI7900, Applied Biosystems, Foster City, CA).

PCR amplification was evaluated using relative quantification by comparison to an internal housekeeping gene (glyceraldehyde 3-phosphate dehydrogenase or GAPDH), which was not affected by treatment. PCR amplification curves were collected using the SDS thermal cycler software package and regressed for their threshold cycle (C_T) using the sigmoidal curve fitting method[55] [SigmaPlot software package (Systat Software, San Jose, CA)]. Relative quantification of gene expression was evaluated using the $\Delta\Delta C_T$ method (as described previously.[61] Serial dilutions of cDNA samples and sigmoidal curve fitting analysis were used to confirm amplification efficiency.

Collagen visualization

Cells-on-glass cover slip samples were removed from culture after 6 and 20 days. Samples were moved to fresh six-well plate, washed twice in phosphate buffered saline (PBS), fixed with Bouin's solution (Richard-Allen Scientific, Kalama-zoo, MI) under ambient conditions for 1 h and rinsed with deionized water to remove excess fixative. Bouin's fixative enhances binding of Picrosirius stain to collagen fiber bundles. Fastgreen stain (0.1%, Sigma) was then used to stain cell layers for 30 min followed by a treatment of glacial acetic acid (American Master Tech Scientific, Lodi, CA) for 30 min to remove excess staining. Fastgreen stains cell layers aniline blue or green with darker color intensity indicating increased tissue density. The Picrosirius stain (American Master Tech Scientific Inc.) was then applied to cell layers for 1 h, followed by a wash with deionized water. A sequential alcohol dehydration (70–100% ethanol) for 30 s followed before imaging. The collagen fiber bundles stained by Picrosirius staining were imaged using polarized light microscopy (due to the birefringent nature of collagen, which appears yellow, orange, or red). An optical microscope (Olympus BX51, Tokyo, Japan) equipped with a CCD camera and Image Pro software was used to capture images of the cell layers under polarized light.

Silicon ion treatments

To determine the influence of ionic silicon on osteoblast function, treatments were made such that the ion concentrations used represented the lowest dissolved ion concentration from ICP-MS results. The source of ionic Si was sodium meta-silicate (Sigma, St. Louis, MO). Additional supplementation of treatments with ascorbic acid and glycerol-2-phosphate were used to make treatments for osteoblasts. Control media was used as described above.

Author Manuscript Author Manuscript Author Manuscript Author Manuscript

OSX siRNA transfection

The siRNA cocktails targeting mouse Sp7/Osterix were purchased from Santa Cruz Biotechnology (Santa Cruz, CA). MC3T3-E1 subclone 4 cells were synchronized with αMEM, 1% FBS, and 1% pen-strep for 48 h. Cells were then transfected using Lipofectamine (Invitrogen) according to the manufacturer's protocol with the transfection agent concentration scaled proportionately to the cell number. After 5–7 h of transfection at 37°C in a CO_2 incubator with growth media (no pen-strep), cells were exposed to 24 h of growth media followed by their respective treatments. Cells were lysed 72 h after the treatments were introduced and analyzed for gene expression using qRT-PCR. Histological analysis for collagen fiber bundle formation was performed 6 days after treatment.

Statistics

Statistical comparison of gene expression results was analyzed using GraphPad Prism 4. Two-way analysis of variance (ANOVA) followed by Bonferroni testing was used for an overall comparison of the independent factors, time and treatment, with the dependent factor, gene expression. For individual and combined ion studies, one-way ANOVA and Tukey's analysis were used for experimental and control comparisons. Statistical comparisons shown are relative to corresponding control group. A power value of $p < 0.05$ was used to report statistical significance. All data analyses were calculated from triplicate sampling per experiment.

RESULTS

Experimental bioactive coating glass ion release kinetics

A generalized kinetic model was used to determine the mass transfer coefficient as it related to bioactive glass ion release. The generalized model (Sepulveda et al.[56]) describes the time-dependent release of ions *in vitro* by,

$$\frac{dc_i}{dt} = kt^{-1/2} \quad (1)$$

where c_i is the ion concentration (ppm or mg L^{-1}), k_i is the overall mass transfer coefficient (ppm $hr^{-½}$or mg L^{-1} $hr^{-½}$), and t is time (hours). The overall mass transfer coefficient, k, depends on many factors including the diffusivity, the glass surface reaction rate constants associated with ion formation, the reaction rate constants involved in the reprecipitation of hydroxyapatite, the degree of super-saturation, the boundary layer thickness, the initial ion concentration, and the diffusion path length.

The ion release from the glass particles follows a diffusion-controlled behavior. At 24–48 h, the release of calcium and phosphate ions reaches an apex [6P53-b: Fig. 1(A,B); 45S5: Fig. 1(C,D)]. The release of Si^{4+} and Mg^{2+} did not reach an apex in ion concentration. The Mg ion release rate had a $t^{-½}$ dependence, giving mass transfer coefficients [according to Eq. (1)] of 1.6 ± 0.1 mg L^{-1} $hr^{-½}$. Similarly, Si ion release had an estimated mass transfer coefficient of 4.5 ± 0.2 mg L^{-1} $hr^{-½}$ (45S5) and 5.0 ±€ 0.1 mg L^{-1} $hr^{-½}$ (6P53-b). In

Author Manuscript Author Manuscript Author Manuscript Author Manuscript

addition, pH measurements showed that the OH^- concentration increased with time, yielding mass transfer coefficients of $6.4 \pm 0.9 \times 10^{-7}$ moles OH^- L^{-1} $h^{-½}$ (6P53-b) and $8.2 \pm 0.9 \times 10^{-7}$ moles OH^- L^{-1} $h^{-½}$ (45S5).

This apex in calcium and phosphate ion concentration caused an increase in the degree of saturation [Fig.1(E,F)]. The increase in these ion concentrations resulted in the degree of saturation, which indicated the favorability of homogeneously or heterogeneously nucleated hydroxyapatite formation.[57,58] As the dissolved ion concentration increased, the degree of saturation also increased.

Effect of GCM treatments on osteoblast-specific gene expression

Growth factors.—Both 45S5 and 6P53-b GCM enhanced growth factor gene expression. For example, the 45S5 GCM markedly enhanced the gene expression of VEGFA in MC3T3-E1 subclone 4 at day 2 (5× control) and day 6 [2× control, Fig. 2(A)]. The gene expression of TGFb1 [Fig. 2(B), 2.5× control] was significantly enhanced in these cells by the 6P53-b GCM treatment at day 6. TGFβ1 involved in the regulation of collagenous and non-collagenous markers during osteogenic differentiation.[59]

Matrix proteins.—The 45S5 GCM enhanced the gene expression levels of CDH11 [Fig. 3(A)], SPP1 [Fig. 3(B), and DMP1 Fig. 3(C)] in MC3T3-E1 subclone 4 cells. Gene expression for CDH11 was four times greater on day 6 and five times greater on day 20 relative to the corresponding controls [Fig. 3(A)]. Similarly, SPP1 gene expression was moderately enhanced on days 6 (2.5× control) and 20 [3.5× control; Fig. 3(B)]. While 45S5 GCM treatment had an impact on the matrix protein DMP1 by 2 fold (day 6), 6P53-b showed a marked enhancement day 20 [16× control, Fig. 3(C)].

Matrix protease.—MMP2 and MMP9 were utilized to study the effect of bioglass ion release on matrix proteinases. The data from MMP2 gene expression showed slight significant differences by both 45S5 and 6P53-b GCM from the control and each other on day 6 [2x, Fig. 4(A)]. Statistical differences were not observed afterward. Conversely, not only were the mRNA levels of MMP9 enhanced by the 45S5 GCM treatment on day 2 (2.5×), but they were markedly upregulated on day 10 by ~25-fold, with a greater enhancement on day 20 (45×) [Fig. 4(B)].

Collagen gene expression.—GCM-treated MC3T3-E1 subclone 4 cells showed increased collagen expression [Col(I)α 1 Fig. 5(A)], Col(I)α2 [Fig. 5(B)]. Compared to control treated cells, Col(I)α1 was significantly enhanced at day 10 for 45S5 GCM treated cells (3× control) and 6P53-b GCM treated cells (1.2× control). For Col(I)α2, its expression was initially enhanced on day 2 (2.0× control) and maximally enhanced in 45S5 GCM-treated cells at 14 days (3.5× control) and at 20 days in 6P53-b GCM treated cells (1.5× control). In addition, continued enhanced collagen expression was observed throughout the time course of the experiment for both GCM treatments. Although not observed in this work, enhancement of Col(I) expression was reported as early as 1 day during differentiation.[30,39]

Author Manuscript Author Manuscript Author Manuscript Author Manuscript

Metalloenzyme expression.—Non-collagenous genes including ALP, LOX, and Sod1 were enhanced in GCM-treated MC3T3-E1 subclone 4 cells. Sod1 expression [Fig. 6(C)] was enhanced in both GCM treatments at day 2 (6P53-b GCM: 2.0× control, 45S5 GCM: 3.5× control). Sod1 is a regulator of collagen cross-linking through the regulation of LOX.[43]

LOX expression [Fig. 6(A)] was also enhanced on day 2 (37× control) and day 20 (25× control) in 45S5 treated cells. For 6P53-b GCM, LOX enhancement occurred after 20 days (2.5× control). Lysyl oxidase is responsible for the cross-linking of collagen fibrils to increase their length.[60]

Alkaline phosphatase, a dephosphorylating enzyme involved in collagen turnover, plays a vital role in the formation of hydroxyapatite and mineralized tissues.[35] Concerning its expression [Fig. 6(B)], 45S5 GCM treatments significantly enhanced its expression on day 2 (3× control), and onward to day 6 (5× control), while 6P53b GCM treated cells had maximal upregulation of ALP on day 6 (3.5× control).

Extracellular matrix collagen formation.—The enhanced gene expression by GCM treatments led to enhanced collagen matrix formation. 45S5 GCM treatments enhanced MC3T3-E1 subclone 4 collagen formation (Fig. 7), which was imaged using polarized light microscopy. 45S5 GCM treatments [Fig. 7(C,F)] exhibited a higher density of orthogonally arranged, elongated collagen fiber bundles as compared to 6P53-b GCM treatments [Fig. 7(B,E)] or control treatments [Fig. 7(A,D)].

Si^{4+} enhances ALP and col(V) expression and collagen synthesis via OSX enhancement—The cells were analyzed for the gene expression of OSX, its down-stream biomarkers (ALP and Col(V)α3), and collagen matrix formation in WT osteoblasts. The results from the gene expression studies of OSX [Fig. 8(A)] showed an increase in OSX mRNA by Si^{4+} treatments vs. control treatments in. Si^{4+} treatments also significantly increased the gene expression of ALP [Fig. 8(B)] and Col(V)α3 [Fig. 8(C)] vs. control treatments. Collagen staining after 6 days post 100 μM silicon treatment [Fig. 8(D)] showed more dense and elongated collagen fibers relative to control [Fig. 8(E)]. These results indicate that Si^{4+} enhances OSX expression, its downstream markers ALP and Col(V), and density of elongated collagen fiber bundles in ECM collagen matrices.

OSX deficiency limits Si^{4+} enhancement of ALP, col(V), and collagen synthesis—Knock-down studies were conducted using siRNA of OSX/Sp7. MC-3T3 cells were treated with control medium and 100 μM Si^{4+} in OSX-null osteoblasts for 3 days. OSX knock-down was first confirmed for both treatments in which siRNA induced a >80% decrease in gene expression of OSX [Fig. 9(A)], OSX-null osteoblasts also showed a significant decreases (≥75%) in mRNA levels of ALP in both treatments [Fig. 9(B)]. Interestingly, although Col(V)α3 mRNA was produced in statistically lower amounts than control treated WT osteoblasts, Col(V)α3 expression was produced in significantly greater amounts in Si^{4+} treated OSX-null cells vs. control treated OSX-null cells [Fig. 9(C)].

An analogous trend was also observed in ECM collagen matrix formation. Both control-treated and Si^{4+}-treated OSX-null cells had a lower density of elongated collagen fiber

Author Manuscript Author Manuscript Author Manuscript Author Manuscript

bundles in ECM as compared to these same treatments in WT osteoblasts. However, the addition of silicon ions to OSX siRNA-treated cells resulted in a greater density of fiber bundles [Fig. 9(D)] compared to the sparse amounts of short extracellular collagen in cells treated with OSX siRNA-alone [Fig. 9(E)]. Overall, these results indicate the dependence of Si^{4+} on OSX expression for the enhancement of ALP and Col(V) expression and collagen matrix formation in osteoblasts.

DISCUSSION

In this study, it was found that the two bioactive glasses studied here (45S5, 6P53-b) enhanced collagen formation during osteogenesis. Several families of growth factors, transcription factors, and enzymes associated with osteogenesis were enhanced. Matrix protein expression of osteocalcin was also enhanced and showed a dependence on glass dosage. Both glasses exhibited similar dissolution behavior (Si^{4+}, Ca^{2+}, PO_4^{3-}) with the exception that 6P53-b released additional Mg^{2+}.

The equilibrium reaction for HA formation is:

$$Ca_{10}(PO_4)_6(OH)_{2(s)} = 10Ca^{2\pm}_{(aq)} \pm 6PO^{3-}_{4(aq)} \pm 2OH^{-}_{(aq)} \quad (2)$$

As the concentrations of these ions increased during glass dissolution (24–48 h), the likelihood of HA formation increased [Fig. 1(E)], which was also observed by Orme et al.[61] Because the likelihood of HA formation was high, this caused the depletion in calcium and phosphate ion concentrations between 48 and 72 h of dissolution. Sepulveda et al.[56] observed a similar trend for 45S5 dissolution after 24 h.

According to the equilibrium constant [Eq. (3)] for the reaction in Eq. (2),

$$K_{SP} = C^{10}_{Ca^{2\pm}} \cdot C^{6}_{PO_4^{3-}} \cdot C^{2}_{OH^-} \cdot \gamma^{10}_{Ca^{2\pm}} \cdot \gamma^{6}_{PO_4^{3-}} \cdot \gamma^{2}_{OH^-}, \quad (3)$$

the ion activities are couple to the ion concentrations that result in a shift in the equilibrium reaction toward HA formation. These ion activities can be described by the well-known Pitzer relation that can be applied to all ions dissolved in the media. This model accounts for short and long range interactions for ions of varying size and charge. This model is valid for media (blood plasma, cell culture media, simulated body fluid) where the ionic strength has been well-documented to be above 0.1 mol kg^{-1} and is considered a saturated solution as shown in Figure 1(E,F). At this ionic strength, the extended Debye–Huckel relation is not valid because of increasing short and long-range interactions with increasing ionic strength.

Si^{4+} release was slower than Ca^{2+} and PO_4^{3-} release, while Mg^{2+} release was even more tepid. These results confirmed the work of Saiz et al. where it was found that Si^{4+} release was approximately an order of magnitude higher than that of Mg^{2+} release.[1] The tepid Mg^{2+} release rate could be owed to (1) increased tendency of chelation within the glass structure

Author Manuscript Author Manuscript Author Manuscript Author Manuscript

owed to the Ca^{2+} and Mg^{2+} presence based on their field electron strength, and (2) the ability of these dopants to slow water molecule ingress through the glass matrix, thus slowing the formation of a hydration layer and improving glass durability.[62,63]

In general, 45S5 GCM treatments enhanced the expression of several osteogenic markers. The enhanced markers included collagens (Col1α1, Col1α2), matrix proteins (DMP1, SPP1, CDH11), growth factors (VEGFA, TGFβ1), and matrix enzymes (LOX, ALP, MMP2, MMP9). This up-regulated effect was probably owed to the presence of Si^{4+} and Ca^{2+}. It is well-known that calcium receptors on cells stimulate many cellular functions including osteogenesis. Thus, the effect of Ca^{2+} on osteogenesis probably acts through this receptor.

In contrast, 6P53-b GCM induced more modest enhancements in the expression of these same osteogenic markers. These modest enhancements were probably owed to the down-regulatory effect of Mg^{2+} in 6P53-b GCM. In this work, it was found that the difference in the ions released by each glass was the release of Mg^{2+} from 6P53-b while all other ion constituencies and concentrations were approximately the same. Moreover, it was found that Mg^{2+} individually down-regulates alkaline phosphatase expression. When Mg^{2+} was combined with Si^{4+} or Ca^{2+}, it was seen to limit their enhanced effects, which probably explains a similar trend when these ions are released together from 6P53-b. Interestingly, 6P53-b GCM did induce a slight up-regulation of Sod1, this did not result in enhanced expression of LOX and collagen matrix fiber bundle density. Thus, Mg^{2+} likely acts as a negative regulator of osteogenic marker expression when released from the bioactive glass matrix.

Yet, the role of Si^{4+} in osteogenesis has not been determined. On the basis of our results, 45S5 GCM had increased density of elongated collagen fiber bundles after 6 days as compared to 6P53-b GCM and control treated osteoblasts. In this work, we isolated the effect of Si^{4+} on osteogenic marker expression involved in ECM collagen formation. When Si^{4+} was added to wild type osteoblasts, it enhanced the expression of osteogenic markers osterix, alkaline phosphatase, and collagen type V. Moreover, we found that the density of collagen matrices was markedly more dense than control treated cells. Because collagen matrices cannot form and alkaline phosphatase and Col(V) depend on osterix expression (as was rationalized above and confirmed in this work), it was hypothesized that Si^{4+} may enhance collagen matrix formation via the osterix pathway.

Upon knockdown of Sp7 (osterix), we found that alkaline phosphatase, and Col(V) expressions were markedly decreased in both control and Si^{4+} treated cells. This contributed to a partial reduction in elongated collagen fiber density. These results indicate that enhanced alkaline phosphatase expression, Col(V) expression, and density of elongated collagen fibers by Si^{4+} depends on enhanced osterix expression. Despite a reduction in the density of elongated collagen fibers, fiber elongation may be dependent on other transcription factors. Other markers that may be present such as Sp1, Runx2, ATF4, or other transcription factors that play a role in osteogenesis may also be involved in collagen fiber elongation. Our future work will focus on resolving this mechanism in full to isolate the specific transcription factor dependence of Si^{4+} enhancement of collagen matrix formation.

Author Manuscript Author Manuscript Author Manuscript Author Manuscript

As an implant coating material, these MgO-doped bioactive glasses may have more specific applications. It may be required that these glasses have a reduced MgO content for their use in bone regeneration. Still, the release of Mg^{2+} from their matrices has some beneficial effects. Mg^{2+} is a regulator of many osteogenic markers involved in bone regeneration, thus, implicating it as an ion more involved in sorbtive properties of bone matrix. In fact, tight regulation of the Ca^{2+}/Mg^{2+} ratio greatly impacts bone regeneration. Thus, as an implant coating, genetic design of the bioactive glasses is important for not only forming new bone around the implant, but enhancing remodeling processes that further strengthen the resultant apposed bone matrix.

CONCLUSIONS

Pertinent to the aims of this study, it was found that bioactive glasses release ions that enhance osteoblast differentiation. These materials control the release of Si and Ca, which were found to enhance collagen gene expression and matrix formation. The enhanced formation of densely packed collagen fiber bundles was attributed to the enhanced expression of regulators of osteogenic collagen fiber crosslinking, elongation, and dephosphorylation. It was also found that Mg release from bioactive glass dampens these enhanced effects by Si and Ca.

ACKNOWLEDGEMENTS

The authors would like to thank the National Institutes of Health/National Institutes for Dental and Craniofacial Research (Grant #R03DE023872, Varanasi, PI) for their support.

Contract grant sponsor: National Institutes of Health/National Institutes for Dental and Craniofacial Research; contract grant number: R03DE023872

REFERENCES

1. Saiz E, Goldman M, Gomez-Vega JM, Tomsia AP, Marshall GW, Marshall SJ. In vitro behavior of silicate glass coatings on Ti6Al4V. Biomaterials 2002;23:3749–3756. [PubMed: 12109700]
2. Arys A, Philippart C, Dourov N, He Y, Le QT, Pireaux JJ. Analysis of titanium dental implants after failure of osseointegration: Combined histological, electron microscopy, and X-ray photoelectron spectroscopy approach. J Biomed Mater Res 1998;43:300–312. [PubMed: 9730068]
3. Jones JD, Saigusa M, VanSickels JE, Tiner BD, Gardner WA. Clinical evaluation of hydroxyapatite-coated titanium plasma-sprayed and titanium plasma-sprayed cylinder dental implants—A preliminary report. Oral Surg Oral Med Oral Pathol Oral Radiol Endodont 1997;84:137–141.
4. Geesink RGT, Hoefnagels NHM. 6-Year results of hydroxyapatite-coated total hip-replacement. J Bone Joint Surg Br Vol 1995;77B: 534–547.
5. Grassmann O, Heimann RB. Compositional and microstructural changes of engineered plasma-sprayed hydroxyapatite coatings on Ti6Al4V substrates during incubation in protein-free simulated body fluid. J Biomed Mater Res 2000;53:685–693. [PubMed: 11074428]
6. Lee TM, Yang CY, Chang E, Tsai RS. Comparison of plasma-sprayed hydroxyapatite coatings and zirconia-reinforced hydroxy-apatite composite coatings: In vivo study. J Biomed Mater Res A 2004;71A:652–660.
7. Teraoka K, Nonami T, Doi Y, Taoda H, Naganuma K, Yokogawa Y, Kameyama T. Hydroxyapatite implantation on the surface of pure titanium for orthopedic implants. Mater Sci Eng C 2000;13:105–107.
8. Pazo A, Saiz E, Tomsia AP. Silicate glass coatings on Ti-based implants. Acta Mater 1998;46:2551–2558.

Author Manuscript Author Manuscript Author Manuscript Author Manuscript

9. Thomas KA, Kay JF, Cook SD, Jarcho M. The effect of surface macrotexture and hydroxylapatite coating on the mechanical strengths and histologic profiles of titanium implant materials. J Biomed Mater Res 1987;21:1395–1414. [PubMed: 3429474]
10. Dhert WJA, Klein CPAT, Wolke JGC, Vandervelde EA, Degroot K, Rozing PM. A mechanical investigation of fluorapatite, magne-siumwhitlockite, and hydroxylapatite plasma-sprayed coatings in goats. J Biomed Mater Res 1991;25:1183–1200. [PubMed: 1667400]
11. Yang CY, Wang BC, Chang WJ, Chang E, Wu JD. Mechanical and histological evaluations of cobalt-chromium alloy and hydroxyapatite plasma-sprayed coatings in bone. J Mater Sci Mater M 1996; 7:167–174.
12. Wang BC, Lee TM, Chang E, Yang CY. The shear-strength and the failure mode of plasma-sprayed hydroxyapatite coating to bone—The effect of coating thickness. J Biomed Mater Res 1993;27: 1315–1327. [PubMed: 8245046]
13. Klein CPAT, Patka P, Vanderlubbe HBM, Wolke JGC, Degroot K. Plasma-sprayed coatings of tetracalciumphosphate, hydroxyl-apatite, and alpha-tcp on titanium-alloy—An interface study. J Biomed Mater Res 1991;25:53–65. [PubMed: 1850430]
14. Hayashi K, Matsuguchi N, Uenoyama K, Kanemaru T, Sugioka Y. Evaluation of metal implants coated with several types of ceramics as biomaterials. J Biomed Mater Res 1989;23:1247–1259. [PubMed: 2606919]
15. Soballe K, Hansen ES, Brockstedtrasmussen H, Pedersen CM, Bunger C. Hydroxyapatite coating enhances fixation of porous coated implants—A comparison in dogs between press fit and noninterference fit. Acta Orthopaed Scand 1990;61:299–306.
16. Weinlaender M, Reumer J, Kenney EB, Moy PK, Adar F. Raman microprobe investigation of the calcium-phosphate phases of 3 commercially available plasma-flame-sprayed hydroxyapatite-coated dental implants. J Mater Sci Mater M 1992;3:397–401.
17. Ji HX, Ponton CB, Marquis PM. Microstructural characterization of hydroxyapatite coating on titanium. J Mater Sci Mater M 1992;3:283–287.
18. Koeneman J, Lemons J, Ducheyne P, Lacefield W, Magee F, Calahan T, Kay J. Workshop on characterization of calcium-phosphate materials. J Appl Biomater 1990;1:79–90.
19. Zyman Z, Weng J, Liu X, Li X, Zhang X. Phase and structural-changes in hydroxyapatite coatings under heat-treatment. Biomaterials 1994;15:151–155. [PubMed: 8011862]
20. Mcpherson R, Gane N, Bastow TJ. Structural characterization of plasma-sprayed hydroxylapatite coatings. J Mater Sci Mater M 1995;6:327–334.
21. Frayssinet P, Tourenne F, Primout I, Delga C, Sergent E, Besse C, Conte P, Guilhem A. A study of structure and degradation of non-polymeric biomaterials implanted in bone using reflected and transmitted light-microscopy. Biotech Histochem 1993;68:333–341. [PubMed: 8292657]
22. Filiaggi MJ, Pilliar RM, Coombs NA. Post-plasma-spraying heat-treatment of the Ha coating/ Ti-6al-4v implant system. J Biomed Mater Res 1993;27:191–198. [PubMed: 8436575]
23. Gross KA, Berndt CC, Goldschlag DD, Iacono VJ. In vitro changes of hydroxyapatite coatings. Int J Oral Maxillofacial Implants 1997; 12:589–597.
24. Hench L. Bioceramics. J Am Ceram Soc 1998;81:1705.
25. Bloyer DR, Gomez-Vega JM, Saiz E, McNaney JM, Cannon RM, Tomsia AP. Fabrication and characterization of a bioactive glass coating on titanium implant alloys. Acta Mater 1999;47:4221–4224.
26. Gomez-Vega JM, Hozumi A, Saiz E, Tomsia AP, Sugimura H, Takai O. Bioactive glass-mesoporous silica coatings on Ti6Al4V through enameling and triblock-copolymer-templated sol–gel processing. J Biomed Mater Res 2001;56:382–389. [PubMed: 11372056]
27. Gomez-Vega JM, Saiz E, Tomsia AP, Marshall GW, Marshall SJ. Bio-active glass coatings with hydroxyapatite and Bioglass (R) particles on Ti-based implants. 1. Processing. Biomaterials 2000;21:105–111. [PubMed: 10632392]
28. Oku T, Suganuma K, Wallenberg LR, Tomsia AP, Gomez-Vega JM, Saiz E. Structural characterization of the metal/glass interface in bioactive glass coatings on Ti-6Al-4V. J Mater Sci Mater M 2001;12:413–417. [PubMed: 15348280]
29. Foppiano S, Marshall SJ, Marshall GW, Saiz E, Tomsia AP. The influence of novel bioactive glasses on in vitro osteoblast behavior. J Biomed Mater Res A 2004;71A:242–249.

Author Manuscript Author Manuscript Author Manuscript Author Manuscript

30. Varanasi VG, Saiz E, Loomer PM, Ancheta B, Uritani N, Ho SP, Tomsia AP, Marshall SJ, Marshall GW. Enhanced osteocalcin expression by osteoblast-like cells (MC3T3-E1) exposed to bioactive coating glass (SiO2-CaO-P2O5-MgO-K2O-Na2O system) ions. Acta Biomater 2009;5:3536–3547. [PubMed: 19497391]
31. Yamauchi M, Yamaguchi T, Kaji H, Sugimoto T, Chihara K. Involvement of calcium-sensing receptor in osteoblastic differentiation of mouse MC3T3-E1 cells. Am J Physiol Endocrinol Metab 2005;288:E608–E616. [PubMed: 15547142]
32. Day RM. Bioactive glass stimulates the secretion of angiogenic growth factors and angiogenesis in vitro. Tissue Eng 2005;11:768–777. [PubMed: 15998217]
33. Mao CM, Yang X, Lu YX, Sun YX, Cheng X, Huang CF. SMAD3 inhibits the expression of MMP-2 in mouse embryonic fibroblasts. Yi Chuan Xue Bao 2005;32:633–640. [PubMed: 16018191]
34. Tamura D, Hiraga T, Myoui A, Yoshikawa H, Yoneda T. Cadherin-11-mediated interactions with bone marrow stromal/osteoblastic cells support selective colonization of breast cancer cells in bone. Int J Oncol 2008;33:17–24. [PubMed: 18575746]
35. Kaji H, Naito J, Sowa H, Sugimoto T, Chihara K. Smad3 differently affects osteoblast differentiation depending upon its differentiation stage. Horm Metab Res 2006;38:740–745. [PubMed: 17111301]
36. Sowa H, Kaji H, Hendy GN, Canaff L, Komori T, Sugimoto T, Chihara K. Menin is required for bone morphogenetic protein 2- and transforming growth factor beta-regulated osteoblastic differentiation through interaction with Smads and Runx2. J Biol Chem 2004;279:40267–40275. [PubMed: 15150273]
37. Beck GR, Zerler B, Moran E. Phosphate is a specific signal for induction of osteopontin gene expression. Proc Natl Acad Sci USA 2000;97:8352–8357. [PubMed: 10890885]
38. Pratap J, Javed A, Languino LR, van Wijnen AJ, Stein JL, Stein GS, Lian JB. The Runx2 osteogenic transcription factor regulates matrix metalloproteinase 9 in bone metastatic cancer cells and controls cell invasion. Mol Cell Biol 2005;25:8581–8591. [PubMed: 16166639]
39. Mosig RA, Dowling O, DiFeo A, Ramirez MCM, Parker IC, Abe E, Diouri J, Aqeel AA, Wylie JD, Oblander SA, Madri J, Bianco P, Apte SS, Zaidi M, Doty SB, Majeska RJ, Schaffler MB, Martignetti JA. Loss of MMP-2 disrupts skeletal and craniofacial development and results in decreased bone mineralization, joint erosion and defects in osteoblast and osteoclast growth. Hum Mol Genet 2007;16:1113–1123. [PubMed: 17400654]
40. Feres-Filho EJ, Menassa GB, Trackman PC. Regulation of lysyl oxidase by basic fibroblast growth factor in osteoblastic MC3T3-E1 cells. J Biol Chem 1996;271:6411–6416. [PubMed: 8626440]
41. Fen JQ, Zhang J, Dallas SL, Lu Y, Chen S, Tan X, et al. Dentin matrix protein 1, a target molecule for Cbfa1 in bone, is a unique bone marker gene. J Bone Miner Res 2002;17:1822–1831. [PubMed: 12369786]
42. Leidi M, Dellera F, Mariotti M, Maier JAM. High magnesium inhibits human osteoblast differentiation in vitro. Magnesium Res 2011;24:1–6.
43. Nojiri H, Saita Y, Morikawa D, Kobayashi K, Tsuda C, Miyazaki T, Saito M, Marumo K, Yonezawa I, Kaneko K, Shirasawa T, Shimizu T. Cytoplasmic superoxide causes bone fragility owing to low-turnover osteoporosis and impaired collagen cross-linking. J Bone Miner Res 2011;26:2682–2694. [PubMed: 22025246]
44. van der Rest M, Garrone R. Collagen family of proteins. FASEB J Off Publ Feder Am Soc Exp Biol 1991;5:2814–2823.
45. Wenstrup RJ, Florer JB, Brunskill EW, Bell SM, Chervoneva I, Birk DE. Type V collagen controls the initiation of collagen fibril assembly. J Biol Chem 2004;279:53331–53337. [PubMed: 15383546]
46. Varanasi VG, Owyoung JB, Saiz E, Marshall SJ, Marshall GW, Loomer PM. The ionic products of bioactive glass particle dissolution enhance periodontal ligament fibroblast osteocalcin expression and enhance early mineralized tissue development. J Biomed Mater Res A 2011;98A:177–184.
47. Hoppe A, Guldal NS, Boccaccini AR. A review of the biological response to ionic dissolution products from bioactive glasses and glass-ceramics. Biomaterials 2011;32:2757–2774. [PubMed: 21292319]

Author Manuscript Author Manuscript Author Manuscript Author Manuscript

48. Hench LL. Genetic design of bioactive glass. J Eur Ceram Soc 2009;29:1257–1265.
49. Varanasi VG, Leong KK, Jue SM, Dominia LM, Loomer PM, Marshall GW. Si and Ca combinatorially target and enhance early MC3T3-E1 osteoblast expression of osteocalcin. J Oral Implantol 2012;38:325–336. [PubMed: 22913306]
50. Nakashima K, Zhou X, Kunkel G, Zhang ZP, Deng JM, Behringer RR, de Crombrugghe B. The novel zinc finger-containing transcription factor Osterix is required for osteoblast differentiation and bone formation. Cell 2002;108:17–29. [PubMed: 11792318]
51. Yoshioka H, Yun-Feng W, Matsuo N, Sumiyoshi H. Sp7/Osterix up-regulates the mouse pro-alpha 3(V) collagen gene (Col5a3) during the osteoblast differentiation. Biochem Biophys Res Commun 2010;394:503–508. [PubMed: 20206127]
52. Matsubara T, Kida K, Yamaguchi A, Hata K, Ichida F, Meguro H, Aburatani H, Nishimura R, Yoneda T. BMP2 regulates osterix through Msx2 and Runx2 during osteoblast differentiation. J Biol Chem 2008;283:29119–29125. [PubMed: 18703512]
53. Zhou X, Zhang Z, Feng JQ, Dusevich VM, Sinha K, Zhang H, Darnay BG, de Crombrugghe B. Multiple functions of Osterix are required for bone growth and homeostasis in postnatal mice. Proc Natl Acad Sci USA 2010;107:12919–12924. [PubMed: 20615976]
54. Kim JE, Baek WY, Lee MA, Jung JW, Kim SY, Akiyama H, de Crombrugghe B. Positive regulation of adult bone formation by osteoblast-specific transcription factor osterix. J Bone Miner Res 2009;24:1055–1065. [PubMed: 19113927]
55. Qiu H, Durand K, Rabinovitch-Chable H, Rigaud M, Gazaille V, Clavere P, Sturtz FG. Gene expression of HIF-1alpha and XRCC4 measured in human samples by real-time RT-PCR using the sig-moidal curve-fitting method. Biotechniques 2007;42:355–362. [PubMed: 17390542]
56. Sepulveda P, Jones JR, Hench LL. In vitro dissolution of melt-derived 45S5 and sol-gel derived 58S bioactive glasses. J Biomed Mater Res 2002;61:301–311. [PubMed: 12007211]
57. Kokubo T, Kushitani H, Ohtsuki C, Sakka S, Yamamuro T. Chemical-reaction of bioactive glass and glass-ceramics with a simulated body-fluid. J Mater Sci Mater M 1992;3:79–83.
58. Larsen MJ. Ion Products and Solubility of Calcium Phosphates Denmark: Royal Dental College; 2001.
59. Harris SE, Bonewald LF, Harris MA, Sabatini M, Dallas S, Feng JQ, Ghoshchoudhury N, Wozney J, Mundy GR. Effects of transforming growth-factor-beta on bone nodule formation and expression of bone morphogenetic protein-2, osteocalcin, osteo-pontin, alkaline-phosphatase, and type-1 collagen messenger-RNA in long-term cultures of fetal-rat calvarial osteoblasts. J Bone Miner Res 1994;9:855–863. [PubMed: 8079661]
60. Byers PH, Siegel RC, Holbrook KA, Narayanan AS, Bornstein P, Hall JG. X-linked cutis laxa: Defective cross-link formation in collagen due to decreased lysyl oxidase activity. N Engl J Med 1980;303:61–65. [PubMed: 6104292]
61. Orme CA, Giocondi JL. Model systems for formation and dissolution of calcium phosphate minerals. In: Behrens P, Bäuerlein E, editors. Chapter 9 in Handbook of Biomineralization Weinheim: Wiley; 2006.
62. Gao H, Tan T, Wang D. Effect of composition on the release kinetics of phosphate controlled release glasses in aqueous medium. J Controlled Release 2004;96:21–28.
63. Gao H, Tan T, Wang D. Dissolution mechanism and release kinetics of phosphate controlled release glasses in aqueous medium. J Controlled Release 2004;96:29–36.

Author Manuscript Author Manuscript Author Manuscript Author Manuscript

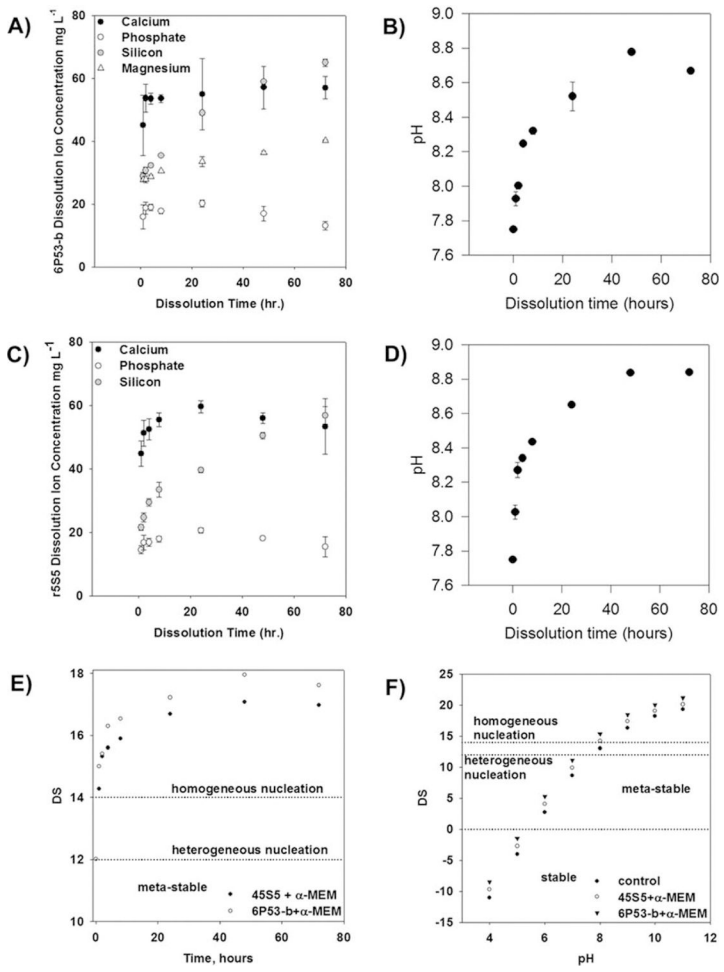

FIGURE 1.

Measurement of ion concentrations for bioactive glass dissolution. (A) Ion concentration and (B) pH measurements [release rate: $6.4 \pm 0.9 \times 10^{-7}$ moles OH– L^{-1} $h^{-½}$.]] for calcium, total phosphate, silicon, and magnesium released from 6P53-b particulates in α-MEM. (C) Ion concentration and (D) pH measurements [($8.2 \pm 0.4 \times 10^{-7}$ moles OH– L^{-1} $h^{2-½}$.)] for calcium, total phosphate, silicon, and magnesium released from 45S5 particulates in α-MEM. (E) Calculations of the degree of saturation (DS) for 45S5 and 6P53-b ion concentrations and (F) 45S5 and 6P53-b GCM and control GCM during *in vitro* cell culture studies (concentrations given in A and C). For DS 5 14, the *in vitro* environment is considered super-saturated and the migration of calcium, phosphate, and hydroxyl ions from the liquid phase to the surface is likely. At DS = 12, the solution is supersaturated, however, heterogeneous nucleation is more likely to occur. For DS < 0, the solution is considered stable and these ions remain soluble.

Author Manuscript Author Manuscript Author Manuscript Author Manuscript

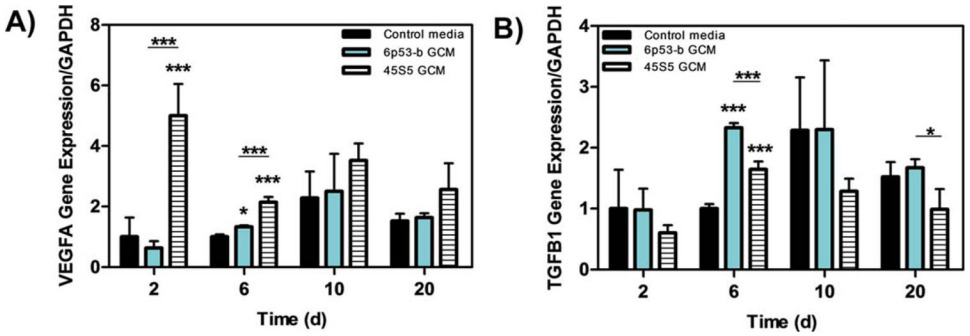

FIGURE 2.

Gene expression of VEGFA and TGFb(I) Effect of 45S5 and 6P53-b GCM on MC3T3-E1 subclone 4 gene expression of (A) vascular endothelial growth factor (VEGFA), and (B) transforming growth factor (TGFb(I)) relative to control treatments. Data presented represent the means ± S.D. of triplicate experiments. Significant differences between treatments were determined by One-Way ANOVA with Dunnett posttest comparison. *$p <$ 0.05, **$p < 0.01$, ***$p < 0.005$ compared to control.

Author Manuscript Author Manuscript Author Manuscript Author Manuscript

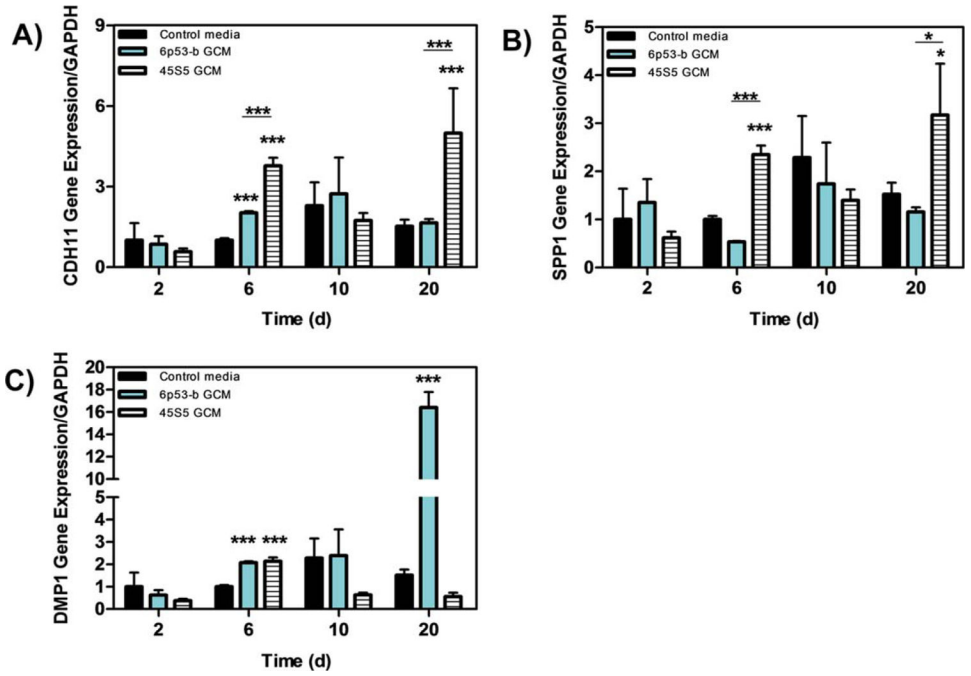

FIGURE 3.

Gene expression of CDH11, SPP1, and DMP1 Effect of 45s5 and 6P53-b GCM on MC3T3-E1 subclone 4 gene expression of (A) cadherin 11 (CDH11), (B) sialo phosphoprotein (SPP1), and (C) dentin matrix protein (DMP1) relative to control treatments. Data presented represent the means ± S.D. of triplicate experiments. Significant differences between treatments were determined by One-Way ANOVA with Dunnett posttest comparison. *$p < 0.05$, **$p < 0.01$, ***$p < 0.005$ compared to control.

Author Manuscript Author Manuscript Author Manuscript Author Manuscript

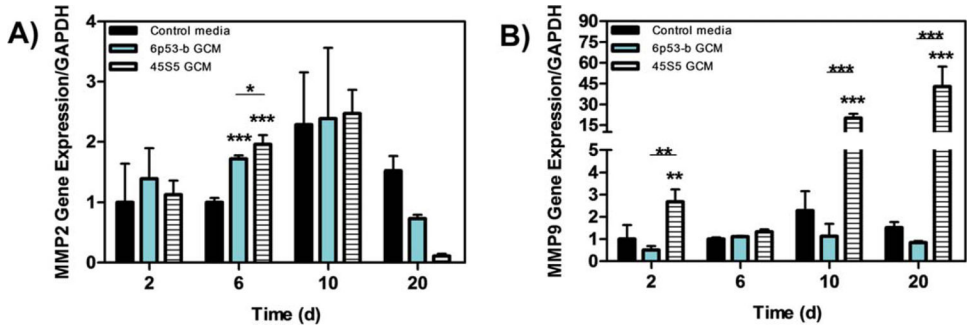

FIGURE 4.

Gene expression of MMP(II) and MMP(IX) Effect of 45s5 and 6P53-b GCM on MC3T3-E1 subclone 4 gene expression of (A) metalomatrix protein II (MMP(II), and (B) metalomatrix protein IX (MMP(IX)) relative to control treatments. Data presented represent the means ± S.D. of triplicate experiments. Significant differences between treatments were determined by One-Way ANOVA with Dunnett posttest comparison. *$p < 0.05$, **$p < 0.01$, ***$p < 0.005$ compared to control.

Author Manuscript Author Manuscript Author Manuscript Author Manuscript

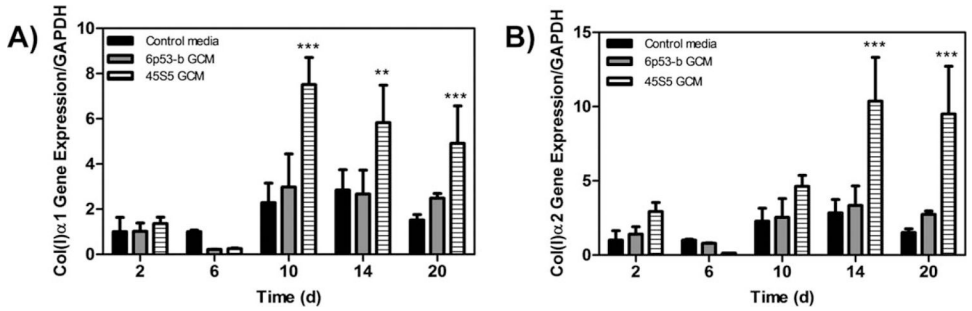

FIGURE 5.

Gene expression of type I collagen effect of 45S5 and 6P53-b GCM treatments on MC3T3-E1 subclone 4 collagen type I collagen expression (Col(I)α1 (A), Col(I)α2 (B)) relative to control treatments. Data presented represent the means ± S.D. of triplicate experiments. Significant differences between treatments were determined by One-Way ANOVA with Dunnett posttest comparison. *$p < 0.05$, **$p < 0.01$, ***$p < 0.005$ compared to control.

Author Manuscript Author Manuscript Author Manuscript Author Manuscript

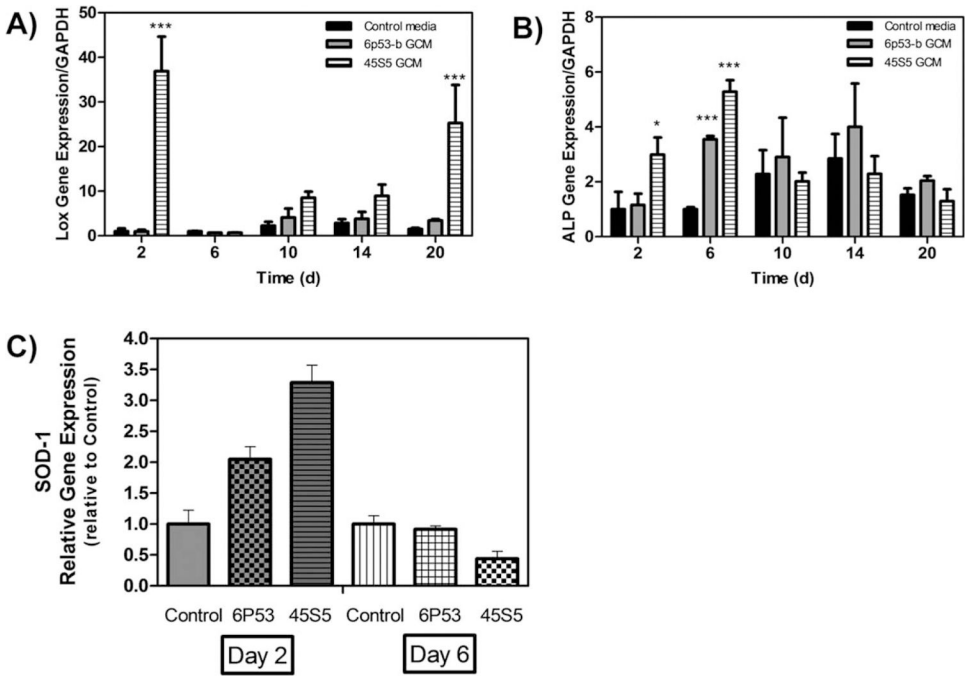

FIGURE 6.

Gene expression of LOX, ALP, and Sod1 Effect of 45S5 and 6P53-b GCM treatments on MC3T3-E1 subclone 4 expression of (A) lysil oxidase (LOX), (B) alkaline phosphatase (ALP), and (C) superoxide dismutase (Sod1) relative to control treatments. Data presented represent the means ± S.D. of triplicate experiments. Significant differences between treatments were determined by one-way ANOVA with Dunnett posttest comparison. $*p < 0.05$, $**p < 0.01$, $***p < 0.005$ compared to control.

Author Manuscript Author Manuscript Author Manuscript Author Manuscript

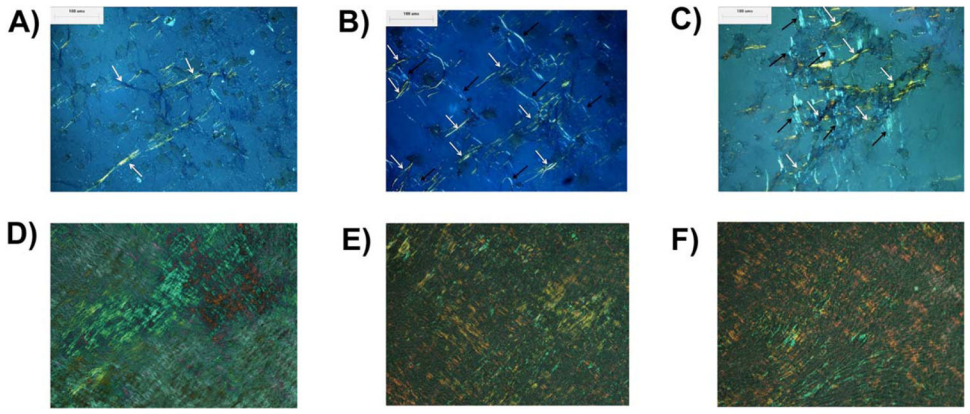

FIGURE 7.

Collagen visualization after 6 days (A–C) and 20 days (D–F) culture Optical micrographs displaying extracellular matrix collagen as a result of MC3T3-E1 subclone 4 exposure to (A), (D) control media + AA + βGP treatment, 6P53-b GCM treatment, (B), (E) and 45S5 GCM treatment, (C), (F) over a 6-day and 20-day period, respectively. White and black arrows indicate elongated collagen fibers aligned in orthogonally oriented layers.

Author Manuscript Author Manuscript Author Manuscript Author Manuscript

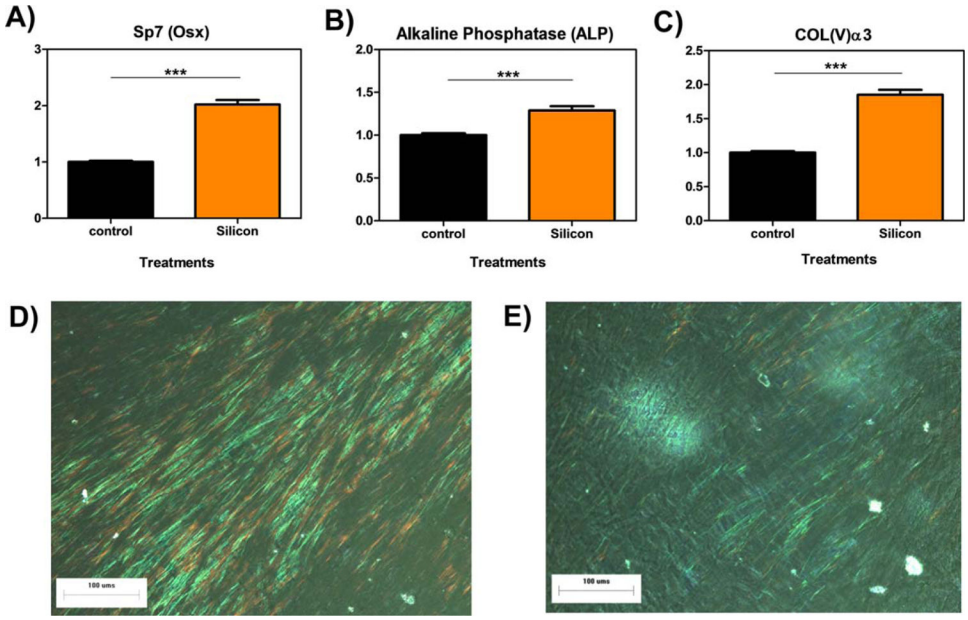

FIGURE 8.

Results of 100 μM Si additive for OSX, ALP, and Col(V)a3 expression and collagen formation. Relative gene expression of OSX, ALP, and Col(V)α3 by MC3T3-E1 subclone 4 cells treated with control media and 100 μM Si for 72 h. Optical micrograph showing extracellular collagen fiber as result of MC3T3-E1 subclone 4 exposure to basal media (D) and 100 μM silicon after 6 days (E). *** indicates $p < 0.005$.

Author Manuscript Author Manuscript Author Manuscript Author Manuscript

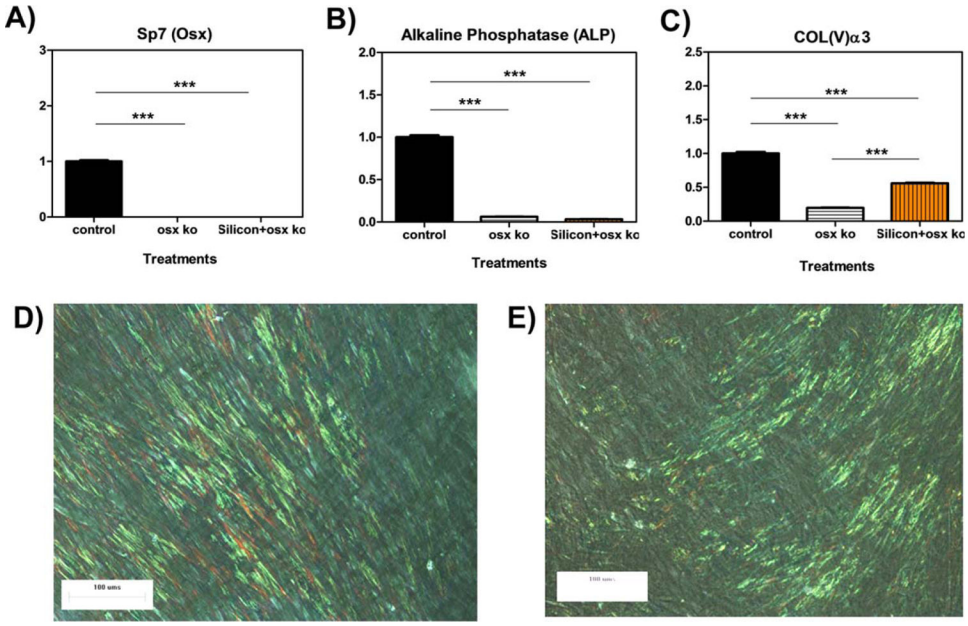

FIGURE 9.

OSX knock-down results for gene expression and collagen formation Relative gene expression of OSX, ALP, and Col(V)α3 by MC3T3-E1 subclone 4 cells treated with control media, OSX siRNA, and 100 μM Si + OSX siRNA for 72 h. Optical micrograph showing extracellular collagen fiber as result of MC3T3-E1 subclone 4 after day 6 post-treatment. MC3T3-E1 subclone 4 cells were exposed to (D) 100 μM silicon + OSX siRNA or (E) OSX siRNA. The presence of fibrillar collagen is seen as the greenish yellow streaks.

Author Manuscript

Author Manuscript

Author Manuscript

Author Manuscript

TABLE I.

Genes Expressed by MC3T3-E1 Subclone 4 Cells During Differentiation

Gene	Name	Primary Function	Reference
Col1α1	Collagen type 1	Provides backbone of bone matrix	31
VEGFA	Vascular endothelial growth factor	Involved in “cross-talk” between osteoblasts and endothelial cells for vascular tissue formation during bone development	32
TGFβ1	Transforming growth factor	Involved in bone metabolism regulation	33
CDH11	Cadherin	Fundamental role for the development and maintenance of bone by mediating cellular crosstalk between osteogenic cells and by For Peer Review providing targets for the sorting and migration of osteogenic precursors toward the bone surface.	34
AKP2	Alkaline Phosphatase	Involved in turnover of collagen type 1 during bone matrix development	35
SMAD1	Smad1	Involved in intracellular signaling during bone development	36
SPP1	Osteopontin	Involved in regulating calcification during bone matrix development	37
MMP9	Matrix metalloprotease	Involved in regulation of growth plate maturation and bone formation	38
MMP2	Matrix metalloprotease	ECM enzyme involved in bone metabolism	39
LOX	Lysyl oxidase	Catalyzes enzymatic step for collagen- elastin cross-linking, which is required for bone formation.	40
DMP1	Dentin matrix Protein	Nuclear transcription factor involved in osteogenic gene expression	41